State-of-the-art nucleon-pair approximation to the nuclear shell model

C. Ma,[1] X. Yin,[1] and Y. M. Zhao[1,2,*]

[1]*Shanghai Key Laboratory of Particle Physics and Cosmology, School of Physics and Astronomy, Shanghai Jiao Tong University, Shanghai 200240, China*

[2]*Collaborative Innovation Center of IFSA (CICIFSA), Shanghai Jiao Tong University, Shanghai 200240, China*

(Received 20 May 2023; revised 19 August 2023; accepted 28 August 2023; published 12 September 2023)

In this paper a state-of-the-art version of the nucleon-pair approximation to the nuclear shell model is suggested. The configuration space is constructed by stepwise coupling collective nucleon pairs with given spin. The one-body and two-body matrix elements, as well as the overlaps, are calculated in terms of the M-scheme nucleon-basis states, without resorting to any angular momentum couplings. Many redundant commutations are avoided by using the Wigner-Eckart theorem and an algorithm similar to the coefficients of fractional parentage in the nuclear shell model calculations. Numerical experiments demonstrate the overwhelming computational superiority in comparison to all previous approaches of nucleon-pair shell model, particularly for the shell model Hamiltonian in the form of effective interactions. In addition, we exemplify this state-of-the-art version of the nucleon-pair approximation by even-even rare-earth $^{142-152}$Nd isotopes, for which the model space is constructed by using *SDGI* nucleon pairs, and the Hamiltonian is adopted as $V_{\text{low-}k}$ potential. Our calculation of the nucleon-pair approximation is able to reproduce reasonably the low-lying energy states of those Nd isotopes, where the seniority-type, vibrational, transitional, and rotational modes are described on the same footing, without adjusting any parameter.

DOI: 10.1103/PhysRevC.108.034308

I. INTRODUCTION

The nuclear shell-model (NSM) [1,2] is the fundamental framework in the nuclear structure theory. However, the NSM suffers from the explosive growth of the configuration space, therefore truncations to the NSM space are indispensable. The nucleon-pair approximation (NPA) to the NSM is one natural and efficient truncation scheme, and along this line we mention the efforts of the generalized seniority scheme [3,4], the broken-pair approximation [5], the fermion dynamical symmetry model [6–8], the multistep shell model [9], and the nucleon-pair shell model [10]. Inspired by the interacting boson model (IBM) [11] and subsequent studies of its microscopic foundation [12–14], the NPA usually constructs the model space by using collective S and D pairs, namely, nucleon pairs with spins 0 and 2, respectively, as analogues of bosons in the IBM. A comprehensive review of the NPA can be found in Ref. [15].

In the last decade, there have been a number of new developments of the NPA. In Ref. [16] the isospin degree of freedom is considered for nucleon pairs, presenting the version of the NPA with isospin; in Ref. [17], nucleon pairs of particle-particle, hole-hole, and particle-hole types are treated on the same footing, presenting the version of the NPA with both valence particles and valence holes, by which one is able to consider the across-shell configurations. These NPA approaches adopt basis states constructed by stepwise couplings of nucleon pairs with given spin; for short we call them the J-scheme versions of the NPA. In contrast to these J-scheme versions, there have been a number of M-scheme approaches: In Ref. [18] the configuration space is constructed in terms of the M-scheme basis of collective nucleon pairs with given spins, and this improvement reduces the CPU time by a factor of 10 for cases with the number of valence-nucleon pairs N larger than 5, in comparison with the traditional approaches [10]. In Ref. [19], the configuration space is constructed by the M-scheme basis, while the commutations of nucleon pairs are represented in terms of matrix products, and this improvement further reduces the CPU cost by a factor of 10 or more for $N \geqslant 4$ in comparison with the version of Ref. [18]. In this paper, for short we refer to the NPA version of Ref. [19] as the M-NPA. All these developments are important for the NPA to be more and more realizable in the studies of heavy nuclei. Yet, the NPA still faces the challenges of CPU cost for systems with more and more valence nucleons and of the complexity due to large dimensions in the M scheme. In addition, in most cases the NPA assumes pairing plus multipole-multipole interactions, and it is very cumbersome to adopt a more general form of the shell model Hamiltonian in the NPA.

It is therefore the purpose of this paper to further develop the NPA, not only substantially saving the CPU cost in comparison with all previous versions of the NPA, e.g., the latest M-scheme versions of the NPA [18,19], but also reserving the elegant simplicity of the traditional NPA in Refs. [10,15]. In addition, by resorting to a technique similar to the coefficients of fractional parentage, computation of matrix elements for a Hamiltonian in the form of effective interactions in this state-of-the-art version of the NPA is as simple as that for the phenomenological pairing plus multipole-multipole interaction.

*Corresponding author:ymzhao@sjtu.edu.cn

This paper is organized as follows. In Sec. II, we explain the NPA basis states, and present reduced matrix elements in the M-NPA. In Sec. III, the matrix elements of one- and two-body operators, and the overlaps between nucleon-pair basis states, are derived for both odd and even systems. In Sec. IV, we elucidate the calculation of nuclear Hamiltonian in this state-of-the-art version of the NPA, for both effective interactions and the phenomenological pairing plus multipole-multipole interactions. In Sec. V, we exemplify this new version of the NPA by using even-even rare-earth $^{142-152}$Nd isotopes to demonstrate the power of our algorithm. Finally, we summarize this paper in Sec. VI.

II. NPA APPROACHES: J SCHEME AND M SCHEME

In this section, we first present the traditional nucleon-pair basis states [10], for completeness; and then we present transformations between those traditional nucleon-pair basis states and those in the M-NPA.

A. Nucleon-pair basis states

In the NSM, a single proton or neutron state can be labeled by quantum numbers n, l, j, and m, where n is the radial number of a spherical oscillator, l the orbital angular momentum, j the total angular momentum, and m the projection of total angular momentum along the principal axis. For short, we abbreviate a single-nucleon creation operator with quantum numbers n_α, l_α, j_α, and m_α by $a^\dagger_{j_\alpha m_\alpha} \equiv a^\dagger_\alpha$. In the case of angular-momentum couplings, m is implicit, and nlj is represented by only j without any confusion.

The traditional NPA employs collective nucleon-pair basis states as building blocks of the configuration space. A collective nucleon pair with spin r and z-axis component m is defined by

$$A^{r\dagger}_m = \sum_{j_1 j_2} y(j_1 j_2 r)\left(a^\dagger_{j_1} \times a^\dagger_{j_2}\right)^{(r)}_m, \tag{1}$$

where j_1, j_2 run over the single-nucleon levels in the valence space. Here, r and m are the spin of the pair and its projection to the principal axis, respectively. The structure coefficients $y(j_1 j_2 r)$ satisfy the symmetry condition

$$y(j_1 j_2 r) = (-)^{j_1+j_2+r+1} y(j_2 j_1 r).$$

In the presence of an even number of valence nucleons, a basis state in the traditional NPA is constructed by successive couplings of collective nucleon pairs, while for a system with an odd number of valence nucleons there is an unpaired nucleon. The NPA basis state is defined as

$$\begin{aligned}|\sigma JM\rangle &= A^{J\dagger}_M(r_0 r_1 r_2 \cdots r_N, J_1 J_2 \cdots J)|0\rangle \\ &= (\cdots((A^{r_0\dagger} \times A^{r_1\dagger})^{(J_1)} \times A^{r_2\dagger})^{(J_2)} \\ &\quad \times \cdots \times A^{r_N\dagger})^{(J)}_M|0\rangle,\end{aligned} \tag{2}$$

where J and M are the total angular momentum of the basis state and its projection, and σ denotes additional quantum numbers of the state. $A^{r_0\dagger} = 1$ for an even system, and $A^{r_0\dagger} = a^\dagger_{j=r_0}$ for an odd system. For short we call the configuration constructed by states in the form of Eq. (2) as the J-NPA basis.

Alternatively, one can construct a basis state without successive couplings of nucleon pairs, as was done in Ref. [18]:

$$|\zeta M\rangle = A^{r_0\dagger}_{m_0} A^{r_1\dagger}_{m_1} A^{r_2\dagger}_{m_2} \cdots A^{r_N\dagger}_{m_N}|0\rangle. \tag{3}$$

Here $M = \sum_{i=0}^N m_i$ and ζ represent additional quantum numbers of the state, and we call the basis states in the form of Eq. (3) the M-NPA basis. Clearly, calculations in the J-NPA basis and the M-NPA basis are equivalent to each other, in the case where all nontrivial intermediate and necessary spins J_i in Eq. (2) and projections m_i in Eq. (3) are properly considered.

B. Transformation between the M-NPA and J-NPA basis states

The transformation between the M-NPA and J-NPA basis states is straightforward in terms of Clebsch-Gordan (CG) coefficients,

$$|\sigma JM\rangle = \sum_\zeta T^{(M)}_{\zeta\sigma}|\zeta M\rangle, \tag{4}$$

where

$$T^{(M)}_{\zeta\sigma} = C^{J_1 M_1}_{r_0 m_0, r_1 m_1} C^{J_2 M_2}_{J_1 M_1, r_2 m_2} \cdots C^{JM}_{J_{N-1} M_{N-1}, r_N m_N},$$

with the requirement that $M_1 = m_0 + m_1$ and $M_i = M_{i-1} + m_i$. It is worthwhile to note that the states represented by Eq. (3) with different ζ are not necessarily independent with each other. States denoted by $\zeta = \{r_0 r_1 \ldots r_N, m_0 m_{i_1} \ldots m_{i_N}\}$, where $\{i_1, \ldots, i_N\}$ represents any permutation of $\{1, \ldots, N\}$, are all the same provided $r_1 = r_2 = \cdots = r_N$. Therefore we need only basis states in which magnetic quantum numbers of identical nucleon pairs are in decreasing or increasing order. Numerical experiments in general cases indicate that the overcompleteness of the nucleon-pair bases is eliminated by considering $|\zeta M\rangle$ without duplication. Consequently, the transformation matrix elements for the pair basis state with the number of $A^{r_i\dagger}$ being n_i is written as

$$\begin{aligned}T^{(M)}_{\zeta\sigma} &= C^{r_0 J_1 \ldots J_{n_1}}_{r_1, m_0 m_1 \ldots m_{n_1}} \times C^{J_{n_1} J_{n_1+1} \ldots J_{n_1+n_2}}_{r_2, M_{n_1} m_{n_1+1} \ldots m_{n_1+n_2}} \\ &\quad \times \cdots \times C^{J_{N-n_l} J_{N-n_l+1} \ldots J_{N-1} J}_{r_l, M_{N-n_l} m_{N-n_l+1} \ldots m_{N-1} m_N},\end{aligned} \tag{5}$$

where $N = \sum_{i=1}^l n_i$ and

$$C^{J_0 J_1 \ldots J_n}_{r, M_0 m_1 \ldots m_n} = \sum_{\{i_1, i_2, \ldots, i_n\}} C^{J_1 M_1}_{J_0 M_0, r m_{i_1}} C^{J_2 M_2}_{J_1 M_1, r m_{i_2}} \cdots C^{J_n M_n}_{J_{n-1} M_{n-1}, r m_{i_n}}. \tag{6}$$

Here $\{i_1, i_2, \ldots, i_n\}$ again denotes all possible permutations of the series $\{1, 2, \ldots, n\}$, and the intermediate projections satisfy the conditions $M_k = M_{k-1} + m_{i_k}$ with k ranging from 1 to n.

C. Reduced matrix elements

In the NSM, the Hamiltonian and physical observables are written in terms of spherical tensor operators, $\hat{O}^t_\mu$, with t and μ here the spin and corresponding z-component projection of the operator.

In this new version of the NPA, the reduced matrix element of $\hat{O}^t$ is calculated by using the Wigner-Echkart theorem, as follows:

$$\begin{aligned}\langle \sigma J \| \hat{O}^t \| \sigma' J' \rangle &= \langle \sigma JM | \hat{O}^t_\mu | \sigma' J' M' \rangle \Big/ C^{JM}_{J'M',t\mu} \\ &= \sum_{\zeta\zeta'} T^{(M)}_{\zeta\sigma} \langle \zeta M | \hat{O}^t_\mu | \zeta' M' \rangle T^{(M')}_{\zeta'\sigma'} \Big/ C^{JM}_{J'M',t\mu}.\end{aligned} \tag{7}$$

In this formula the reduced matrix elements $\langle \sigma J \| \hat{O}^t \| \sigma' J' \rangle$ are given in terms of the matrix elements $\langle \sigma JM | \hat{O}^t_\mu | \sigma' J' M' \rangle$ and Clebsch-Gordan coefficient $C^{JM}_{J'M',t\mu}$, and this is one of the advantages of J-NPA: In the M-NPA [18,19], one actually has to calculate matrix elements with all possible magnetic numbers; while in Eq. (7) one needs the M-NPA matrix elements for only one set of arbitrary projections M, μ, and M'. Interesting issues related to the particular choice of M, μ, and M', are given in Appendix A.

III. MATRIX ELEMENTS

In this section, we derive the matrix elements of one-body and two-body operators, and overlaps in our new approach of the NPA. For short we adopt the Einstein summation convention using subscripts of greek letters.

A. One- and two-body operators

In all previous versions of the NPA, one calculates the matrix element of an operator in an explicit manner, namely, in the complete form of very complicated summations. Here in this new version of the NPA, we present the results of one- and two-body operators in a factorial form.

A general one- and two-body operators in the uncoupled representation are defined as

$$\hat{Q} = q_{\alpha\beta} a^\dagger_\alpha a_\beta, \tag{8}$$

$$\hat{\mathcal{O}} = o_{\alpha\beta\gamma\delta} a^\dagger_\alpha a^\dagger_\beta a_\delta a_\gamma, \tag{9}$$

where the structure coefficients $q_{\alpha\beta}$ construct a matrix q. The structure coefficients $o_{\alpha\beta\gamma\delta}$ form a four-dimensional tensor o, with antisymmetry of changing the first or last two indices:

$$o_{\alpha\beta\gamma\delta} = -o_{\beta\alpha\gamma\delta} = -o_{\alpha\beta\delta\gamma} = o_{\beta\alpha\delta\gamma}. \tag{10}$$

According to Ref. [19], a matrix element in the M-NPA can be represented as a number of traces and matrix products of the structure coefficients. Therefore, the matrix element of an operator is a linear superposition of its structure coefficients. For one- and two-body operators, we have

$$\langle \zeta' M' | \hat{Q} | \zeta M \rangle = f_{\alpha\beta} q_{\alpha\beta}, \tag{11}$$

$$\langle \zeta' M' | \hat{\mathcal{O}} | \zeta M \rangle = g_{\alpha\beta\gamma\delta} o_{\alpha\beta\gamma\delta}, \tag{12}$$

with $f_{\alpha\beta}$ and $g_{\alpha\beta\gamma\delta}$ defined by

$$f_{\alpha\beta} = \langle \zeta' M' | a^\dagger_\alpha a_\beta | \zeta M \rangle, \tag{13}$$

$$g_{\alpha\beta\gamma\delta} = \langle \zeta' M' | a^\dagger_\alpha a^\dagger_\beta a_\delta a_\gamma | \zeta M \rangle. \tag{14}$$

In principle, one might use Eqs. (34)–(35) and (38)–(39) in Ref. [19] to calculate $f_{\alpha\beta}$ and $g_{\alpha\beta\gamma\delta}$. However, such computations involve of a huge number of redundant recursions. Below we propose a novel approach to calculate $f_{\alpha\beta}$ and $g_{\alpha\beta\gamma\delta}$.

B. Uncoupled basis states and their contractions

We begin with the uncoupled representation of the basis states. In that case a general nucleon-pair creator is defined as

$$P^\dagger_i = p^{(i)}_{\alpha\beta} a^\dagger_\alpha a^\dagger_\beta, \tag{15}$$

where $p^{(i)}_{\alpha\beta}$ are the structure coefficients of a pair with antisymmetry $p^{(i)}_{\alpha\beta} = -p^{(i)}_{\beta\alpha}$. In an odd-nucleon system, an unpaired-nucleon creator is represented by a linear combination of single-nucleon states:

$$a^\dagger = s_\alpha a^\dagger_\alpha, \tag{16}$$

with s_α the structure coefficients of the unpaired nucleon. Here, $p^{(i)}_{\alpha\beta}$ and s_α correspond to a matrix p_i and a column vector s, respectively. By defining $p^{(i)}_{\alpha\beta} = y(j_\alpha j_\beta r_i) C^{r_i m_i}_{j_\alpha m_\alpha, j_\beta m_\beta}$ and $s_\alpha = \delta_{j_\alpha r_0} \delta_{m_\alpha m_0}$, the M-NPA basis state of Eq. (3) is rewritten as

$$|\zeta M\rangle = P^\dagger_0 P^\dagger_1 \cdots P^\dagger_N |\rangle, \tag{17}$$

with

$$P^\dagger_0 = \begin{cases} 1 & \text{in even systems,} \\ a^\dagger & \text{in odd systems.} \end{cases}$$

In order to calculate $f_{\alpha\beta}$ and $g_{\alpha\beta\gamma\delta}$, we use fundamental commutative relations as below:

$$[A, B_1 B_2 \cdots B_N] = \sum_{k=1}^{N} B_1 \cdots B_{k-1} [A, B_k] B_{k+1} \cdots B_N, \tag{18}$$

where A and B_k are arbitrary operators. The commutators have been derived extensively in Refs. [19,20], and here we cite some basic commutators given in Ref. [19]:

$$\begin{aligned}
&[P_1, P^\dagger_2] = -2\mathrm{tr}(p_2 p_1) + \hat{Q}_1 \quad \text{with} \quad q_1 = 4(p_2 p_1), \\
&[\hat{Q}_2, P^\dagger_3] = P^\dagger_4 \quad \text{with} \quad p_4 = q_2 p_3 + p_3 q_2^\top, \\
&[a_1, P^\dagger_5] = a^\dagger_2 \quad \text{with} \quad s_2 = 2(s_1^\top p), \\
&[\hat{Q}_3, a^\dagger_3] = a^\dagger_4 \quad \text{with} \quad s_4 = q_3 s_3, \\
&\{a_5, a^\dagger_6\} = \{a^\dagger_6, a_5\} = s_5^\top s_6,
\end{aligned} \tag{19}$$

where p_k and q_k are the structure matrices of $P^\dagger_k$ and $\hat{Q}_k$, respectively, and s_k are the structure arrays of $a^\dagger_k$. The superscript $\top$ means the transposition of matrix or column array. Using Eqs. (18) and (19), an uncoupled basis state can be

contracted by $\mathbb{N}$ pairs of annihilators as follows:

$$\begin{aligned} P'_0P'_1\cdots P'_{\mathbb{N}}|\zeta M\rangle &= P'_0P'_1\cdots P'_{\mathbb{N}}P^\dagger_0P^\dagger_1\cdots P^\dagger_N|0\rangle = P'_0P'_1\cdots P'_{\mathbb{N}-1}[P'_{\mathbb{N}},P^\dagger_NP^\dagger_{N-1}\cdots P^\dagger_0]|0\rangle \\ &= \sum_{k=1}^{N} P'_0\cdots P'_{\mathbb{N}-1}P^\dagger_0\cdots P^\dagger_{k-1}P^\dagger_{k+1}\cdots P^\dagger_{N-1}\mathscr{P}^\dagger_k|0\rangle \\ &+ \sum_{k=1}^{N}\sum_{i=1}^{k-1} P'_0\cdots P'_{\mathbb{N}-1}P^\dagger_0\cdots P^\dagger_{i-1}P^\dagger_{i+1}\cdots P^\dagger_{k-1}P^\dagger_{k+1}\cdots P^\dagger_N\mathscr{P}^\dagger_{i,k}|0\rangle \\ &+ \sum_{k=1}^{N} P'_0\cdots P'_{\mathbb{N}-1}a^\dagger_kP^\dagger_1\cdots P^\dagger_{k-1}P^\dagger_{k+1}\cdots P^\dagger_N|0\rangle|_{\text{odd syst.}}, \end{aligned} \tag{20}$$

where the last term with subscript "odd syst." corresponds to the odd-proton or odd-neutron systems and thus vanishes for even-even cases, and we use this convention throughout this paper. The structure coefficients of $\mathscr{P}^\dagger_k$, $\mathscr{P}^\dagger_{i,k}$, and $a^\dagger_k$ are

$$\begin{aligned} \mathfrak{p}_k &= -2\text{tr}(p_kp'_{\mathbb{N}})p_N, \\ \mathfrak{p}_{i,k} &= 4(p_kp'_{\mathbb{N}}p_i + p_ip'_{\mathbb{N}}p_k), \\ s_k &= 4(p_kp'_{\mathbb{N}}s). \end{aligned}$$

This formula is applicable to both odd number and even number of systems, and can be applied recursively until all possible commutations are exhausted.

In the case of $N-\mathbb{N}=2$, the righ-hand side of Eq. (20) corresponds to the "quartet" wave function.

$$P'_0P'_1\cdots P'_{N-2}|\zeta M\rangle = \sum_{\{\xi,\varsigma\}}\mathscr{P}^\dagger_\xi\mathscr{P}^\dagger_\varsigma|0\rangle = \mathcal{Q}^\dagger|0\rangle. \tag{21}$$

Here structure matrices of collective pairs $\mathfrak{p}_\xi$ and $\mathfrak{p}_\varsigma$, are derived via the recursive procedures of Eq. (20), therefore the structure coefficients of the quartet wave function, $\mathcal{Q}^\dagger|0\rangle$, are as follows:

$$\mathfrak{q}_{\alpha\beta\gamma\delta} = \sum_{\{\xi,\varsigma\}}\mathfrak{p}^{(\xi)}_{\alpha\beta}\mathfrak{p}^{(\varsigma)}_{\gamma\delta}. \tag{22}$$

According to the Pauli principle, the structure coefficients of $\mathcal{Q}^\dagger$ equal

$$\begin{aligned} \bar{\mathfrak{q}}_{\alpha\beta\gamma\delta} = \tfrac{1}{6}(&\mathfrak{q}_{\alpha\beta\gamma\delta} - \mathfrak{q}_{\alpha\gamma\beta\delta} + \mathfrak{q}_{\alpha\delta\beta\gamma} \\ &+ \mathfrak{q}_{\beta\gamma\alpha\delta} - \mathfrak{q}_{\beta\delta\alpha\gamma} + \mathfrak{q}_{\gamma\delta\alpha\beta}), \end{aligned} \tag{23}$$

and follow the antisymmetry as below:

$$\bar{\mathfrak{q}}_{\alpha\beta\gamma\delta} = (-1)^{N_{\text{inv}}}\bar{\mathfrak{q}}_{i_\alpha i_\beta i_\gamma i_\delta}, \tag{24}$$

where the indices $\{i_\alpha, i_\beta, i_\gamma, i_\delta\}$ represents any permutation of $\{\alpha,\beta,\gamma,\delta\}$, and N_{inv} denotes the inversion number in this permutation.

In the case of $N-\mathbb{N}=1$, the results are similar:

$$\begin{aligned} P'_0P'_1\cdots P'_{N-1}|\zeta M\rangle &= P'_{N-1}P'_0P'_1\cdots P'_{N-2}|\zeta M\rangle \\ &= P'_{N-1}\mathcal{Q}^\dagger|0\rangle = \mathcal{B}^\dagger|0\rangle. \end{aligned} \tag{25}$$

The last step of the above formula means that the final result, $\mathcal{B}^\dagger|0\rangle$, is obtained by commutation between P'_{N-1} and $\mathcal{Q}^\dagger$ in Eq. (21). The structure coefficients of $\mathcal{B}^\dagger$ are given by

$$b_{\alpha\beta} = 12\,p'^{(N-1)}_{\gamma\delta}\bar{\mathfrak{q}}_{\alpha\beta\gamma\delta}. \tag{26}$$

The factor 12 originates from the different choices of indices in $\bar{\mathfrak{q}}$ to be summed. The antisymmetry condition $b_{\alpha\beta}=-b_{\beta\alpha}$ is satisfied using this expression.

One useful case of Eq. (20) is that of an odd system contracted by $N-1$ annihilating pair operators, which yields a "triad" state,

$$\begin{aligned} P'_1\cdots P'_{N-1}|\zeta M\rangle|_{\text{odd syst.}} &= \sum_{\{\xi,\varsigma\}}a^\dagger_\xi\mathscr{P}^\dagger_\varsigma|0\rangle \\ &= \mathcal{T}^\dagger|0\rangle \equiv \sum_{\alpha\beta\gamma}\mathfrak{t}_{\alpha\beta\gamma}a^\dagger_\alpha a^\dagger_\beta a^\dagger_\gamma|0\rangle, \end{aligned} \tag{27}$$

where structure arrays s_ξ and the structure matrices $\mathfrak{p}_\varsigma$ on the right-hand side of the first identity symbol are calculated by using Eq. (20), and structure coefficients of $\mathcal{T}^\dagger$, i.e., $\mathfrak{t}_{\alpha\beta\gamma}$, are given by

$$\mathfrak{t}_{\alpha\beta\gamma} = \sum_{\{\xi,\varsigma\}}s^{(\xi)}_\alpha\mathfrak{p}^{(\varsigma)}_{\beta\gamma}. \tag{28}$$

Again, coefficients $\mathfrak{t}_{\alpha\beta\gamma}$ of $\mathcal{T}^\dagger$ are

$$\bar{\mathfrak{t}}_{\alpha\beta\gamma} = \tfrac{1}{3}(\mathfrak{t}_{\alpha\beta\gamma} - \mathfrak{t}_{\beta\alpha\gamma} + \mathfrak{t}_{\gamma\alpha\beta}), \tag{29}$$

and follow the antisymmetry

$$\bar{\mathfrak{t}}_{\alpha\beta\gamma} = (-1)^{N_{\text{inv}}}\bar{\mathfrak{t}}_{i_\alpha i_\beta i_\gamma}. \tag{30}$$

For an odd system, $\mathcal{B}^\dagger$ can also be obtained through commutator of P'_0 and $\mathcal{T}^\dagger$, and its structure coefficients are

$$b_{\alpha\beta} = 3s'_\gamma\bar{\mathfrak{t}}_{\alpha\beta\gamma}, \tag{31}$$

where s' is the structure array of the odd nucleon P'_0.

C. Formulation of noncollective matrix elements and overlaps

We present the formulas of $f_{\alpha\beta}$ and $g_{\alpha\beta\gamma\delta}$ as follows. For $g_{\alpha\beta\gamma\delta}$, we have

$$\begin{aligned}
g_{\alpha\beta\gamma\delta} &\equiv \langle 0|P'_0P'_1\cdots P'_N a^\dagger_\alpha a^\dagger_\beta a_\delta a_\gamma|\zeta M\rangle = \langle 0|[P'_0P'_1\cdots P'_N, a^\dagger_\alpha a^\dagger_\beta]a_\delta a_\gamma|\zeta M\rangle \\
&= 2\sum_{k=1}^{N} p'^{(k)}_{\alpha\beta}\langle 0|a_\delta a_\gamma P'_0\cdots P'_{k-1}P'_{k+1}\cdots P'_N|\zeta M\rangle + 4\sum_{k=1}^{N}\sum_{i=1}^{k-1}\left[p'^{(k)}_{\alpha\alpha'}p'^{(i)}_{\beta'\beta} + p'^{(i)}_{\alpha\alpha'}p'^{(k)}_{\beta'\beta}\right]\langle 0|a_\delta a_\gamma a_{\beta'}a_{\alpha'} \\
&\quad\times P'_0\cdots P'_{i-1}P'_{i+1}\cdots P'_{k-1}P'_{k+1}\cdots P'_N|\zeta M\rangle + 2\sum_{k=1}^{N}\left[s'_\alpha p'^{(k)}_{\beta\alpha'} - s'_\beta p'^{(k)}_{\alpha\alpha'}\right]\langle 0|a_\delta a_\gamma a_{\alpha'}P'_1\cdots P'_{k-1}P'_{k+1}\cdots P'_N|\zeta M\rangle|_{\text{odd syst.}} \\
&= 2\sum_{k=1}^{N} p'^{(k)}_{\alpha\beta}\langle 0|a_\delta a_\gamma \mathcal{B}^\dagger_k|0\rangle + 4\sum_{k=1}^{N}\sum_{i=1}^{k-1}\left[p'^{(k)}_{\alpha\alpha'}p'^{(i)}_{\beta'\beta} + p'^{(i)}_{\alpha\alpha'}p'^{(k)}_{\beta'\beta}\right]\langle 0|a_\delta a_\gamma a_{\beta'}a_{\alpha'}\mathcal{Q}^\dagger_{i,k}|0\rangle \\
&\quad + 2\sum_{k=1}^{N}\left[s'_\alpha p'^{(k)}_{\beta\alpha'} - s'_\beta p'^{(k)}_{\alpha\alpha'}\right]\langle 0|a_\delta a_\gamma a_{\alpha'}\mathcal{T}^\dagger_k|0\rangle|_{\text{odd syst.}} \\
&= 4\sum_{k=1}^{N} p'^{(k)}_{\alpha\beta}b^{(k)}_{\gamma\delta} + 96\sum_{k=1}^{N}\sum_{i=1}^{k-1}\left[p'^{(k)}_{\alpha\alpha'}\bar{\mathfrak{q}}^{(i,k)}_{\alpha'\beta'\gamma\delta}p'^{(i)}_{\beta'\beta} + p'^{(i)}_{\alpha\alpha'}\bar{\mathfrak{q}}^{(i,k)}_{\alpha'\beta'\gamma\delta}p'^{(k)}_{\beta'\beta}\right] + 12\sum_{k=1}^{N}\left[s'_\alpha p'^{(k)}_{\beta\alpha'} - s'_\beta p'^{(k)}_{\alpha\alpha'}\right]\bar{\mathfrak{t}}^{(k)}_{\alpha'\gamma\delta}|_{\text{odd syst.}}.
\end{aligned} \tag{32}$$

The factors 4, 12, and 96, on the right-hand of the above formula, originate from permutation symmetry. Structure coefficients $\bar{\mathfrak{q}}_{i,k}$ and $\bar{\mathfrak{t}}_k$ are calculated by using Eq. (20), and are symmetrized by using Eqs. (23) and (29). We note that, according to Eqs. (26) and (31), the structure coefficients b_k can be obtained arbitrarily from either one of $\bar{\mathfrak{q}}_{i,k}$ by $b^{(k)}_{\alpha\beta} = 12p'^{(i)}_{\gamma\delta}\bar{\mathfrak{q}}^{(i,k)}_{\alpha\beta\gamma\delta}$ or one of $\bar{\mathfrak{t}}_k$ by $b^{(k)}_{\alpha\beta} = 12s'_\gamma\bar{\mathfrak{t}}^{(k)}_{\alpha\beta\gamma}$.

For $f_{\alpha\beta}$, we have

$$\begin{aligned}
f_{\alpha\beta} &= \langle 0|P'_0P'_1\cdots P'_N a^\dagger_\alpha a_\beta|\zeta M\rangle = \langle 0|[P'_0P'_1\cdots P'_N, a^\dagger_\alpha a_\beta]|\zeta M\rangle \\
&= \sum_{k=1}^{N} 2p'^{(k)}_{\alpha\gamma}\langle 0|a_\gamma a_\beta P'_0\cdots P'_{k-1}P'_{k+1}\cdots P'_N|\zeta M\rangle + s'_\alpha\,\langle 0|a_\beta P'_N P'_1\cdots P'_{N-1}|\zeta M\rangle\big|_{\text{odd syst.}} \\
&= \sum_{k=1}^{N} 2p'^{(k)}_{\alpha\gamma}\langle 0|a_\gamma a_\beta \mathcal{B}^\dagger_k|\rangle + s'_\alpha\,\langle 0|a_\beta P'_N\mathcal{T}^\dagger_N|0\rangle\big|_{\text{odd syst.}} \\
&= \sum_{k=1}^{N} 4(p'_k b^\top_k)_{\alpha\beta} + 6\,s'_\alpha\bar{\mathfrak{t}}^{(N)}_{\beta\gamma\delta}p'^{(N)}_{\gamma\delta}\big|_{\text{odd syst.}}.
\end{aligned} \tag{33}$$

In addition to the matrix elements $g_{\alpha\beta\gamma\delta}$ and $f_{\alpha\beta}$, the overlap between the two basis states can also be formulated using b_N as

$$\begin{aligned}
\langle\zeta' M'|\zeta M\rangle &= \langle 0|P'_0P'_1\cdots P'_N|\zeta M\rangle = p^{(N)}_{\alpha\beta}\langle 0|a_\beta a_\alpha P'_0\cdots P'_{N-1}|\zeta M\rangle \\
&= p^{(N)}_{\alpha\beta}\langle 0|a_\beta a_\alpha\mathcal{B}^\dagger_N|0\rangle = -2\,\mathrm{tr}(p_N b_N).
\end{aligned} \tag{34}$$

IV. APPLICATION TO SHELL MODEL HAMILTONIAN

In this section we discuss the shell model Hamiltonian $\hat{H}$, and decompose it into operators defined in Eqs. (8) and (9). Once the structure coefficients, $q_{\alpha\beta}$ and $o_{\alpha\beta\gamma\delta}$, of these operators are given, one can easily calculate the matrix elements of $\hat{H}$ in the nucleon-pair configuration space by using the formulas in the last section. In this section we also use numerical experiments to demonstrate the computational power of this state-of-the-art version of the NPA.

A. Effective interactions

The general form of $\hat{H}$ with effective interactions is expressed with good isospin, corresponding to

$$\hat{H} = \sum_j \varepsilon_j N_j + \sum_{\substack{j_\alpha\leqslant j_\beta\\ j_\gamma\leqslant j_\delta}}\sum_{JM}\sum_{TM_T}\frac{V_{JT}(j_\alpha j_\beta j_\gamma j_\delta)}{\sqrt{(1+\delta_{j_\alpha j_\beta})(1+\delta_{j_\gamma j_\delta})}}A^{JT\dagger}_{MM_T}(j_\alpha j_\beta)A^{JT}_{MM_T}(j_\gamma j_\delta), \tag{35}$$

where $N_j = \sum_{m\tau} a^\dagger_{jm\frac{1}{2}\tau} a_{jm\frac{1}{2}\tau}$, and

$$A^{JT\dagger}_{MM_T}(j_\alpha j_\beta) = \sum_{\substack{m_\alpha m_\beta \\ \tau_\alpha \tau_\beta}} C^{JM}_{j_\alpha m_\alpha, j_\beta m_\beta} C^{TM_T}_{\frac{1}{2}\tau_\alpha, \frac{1}{2}\tau_\beta} a^\dagger_{j_\alpha m_\alpha \frac{1}{2}\tau_\alpha} a^\dagger_{j_\beta m_\beta \frac{1}{2}\tau_\beta}.$$

$V_{JT}(j_\alpha j_\beta j_\gamma j_\delta)$ in Eq. (35) represents the two-body matrix elements $V_{JT}(j_\alpha j_\beta j_\gamma j_\delta)$, which take, in the first step, the matrix elements based on realistic nuclear force as corresponding initial values, and then in the second step are refined by optimizing these matrix elements to achieve a best agreement with experimental data.

In the NPA calculations, the Hamiltonian $\hat{H}$ is rewritten in three parts, the proton part, neutron part, and proton-neutron part, which are as follows:

$$\hat{H} = \hat{H}_{\pi\nu} + \sum_{\eta=\pi,\nu} \hat{H}_\eta, \quad \hat{H}_{\pi\nu} = \sum_{i,t} V^{\pi\nu}_{i,t} (-)^t \sqrt{2t+1} \big(\hat{Q}^{i,t}_\pi \times \hat{Q}^{i,t}_\nu\big)^{(0)}, \quad \hat{Q}^{i,t}_{\eta,\mu} = \sum_{j_\alpha j_\beta} q_{\eta,i}(j_\alpha j_\beta t)(a^\dagger_{\eta,j_\alpha} \times \tilde{a}_{\eta,j_\beta})^t_\mu,$$

$$\hat{H}_\eta = \sum_\alpha \varepsilon_{j_\alpha} a^{\eta\dagger}_\alpha a^\eta_\alpha + \sum_{\substack{j_\alpha \leqslant j_\beta \\ j_\gamma \leqslant j_\delta}} \sum_J \frac{V_{JT=1}(j_\alpha j_\beta j_\gamma j_\delta)}{\sqrt{(1+\delta_{j_\alpha j_\beta})(1+\delta_{j_\gamma j_\delta})}} \sqrt{2J+1} \big[A^{J\dagger}_\eta(j_\alpha j_\beta) \times \tilde{A}^J_\eta(j_\gamma j_\delta)\big]^{(0)}, \tag{36}$$

with $\tilde{A}^J_M = (-)^{J-M} A^J_{-M}$, and index i is used to distinguish one-body operators with same spin number t and different structure coefficients. Structure coefficients of $\hat{Q}^{i,t}_{\eta,\mu}$ satisfy a sum rule for the index i,

$$\sum_i q_{\pi,i}(j_\alpha j_\beta t) V^{\pi\nu}_{i,t} q_{\nu,i}(j_\gamma j_\delta t) = \sum_J (-)^{J+j_\gamma+j_\beta} \frac{2J+1}{2} \begin{Bmatrix} j_\alpha & j_\gamma & J \\ j_\delta & j_\beta & t \end{Bmatrix} \sum_{T=0,1} V_{JT}(j_\alpha j_\gamma j_\beta j_\delta) \sqrt{(1+\delta_{j_\alpha j_\gamma})(1+\delta_{j_\beta j_\delta})}. \tag{37}$$

To calculate the matrix element of $\hat{H}_\eta$, we treat it as a one-body operator $\hat{Q}$ plus two-body operator $\hat{\mathcal{O}}$, and fix the structure coefficients in Eqs. (8) and (9) as

$$\begin{aligned} q_{\alpha\beta} &= \delta_{\alpha\beta}\varepsilon_{j_\alpha}, \\ o_{\alpha\beta\gamma\delta} &= \sum_J \frac{\sqrt{(1+\delta_{j_\alpha j_\beta})(1+\delta_{j_\gamma j_\delta})}}{4} V_{JT=1}(j_\alpha j_\beta j_\gamma j_\delta) C^{J\,m_\alpha+m_\beta}_{j_\alpha m_\alpha, j_\beta m_\beta} C^{J\,m_\alpha+m_\beta}_{j_\gamma m_\gamma, j_\delta m_\delta}. \end{aligned} \tag{38}$$

For $\hat{H}_{\pi\nu}$, those of one-body operators $\hat{Q}^{i,t}_{\eta,\mu}$ are written as follows:

$$q^{(i)}_{\alpha\beta} = (-)^{j_\beta+m_\beta} q_{\eta,i}(j_\alpha j_\beta t) C^{t\mu}_{j_\alpha m_\alpha, j_\beta -m_\beta}. \tag{39}$$

Now it is practical to calculate the (reduced) matrix elements of corresponding operators using formulas in the previous sections, and accordingly derive the reduced matrix elements of $\hat{H}$ as in the J-NPA approach.

B. Phenomenological interactions

In the case that $\hat{H}$ takes the form of pairing forces and multipole-multipole interactions [21], we have

$$\begin{aligned} \hat{H} &= \hat{H}_{\pi\nu} + \sum_{\eta=\pi,\nu} \hat{H}_\eta, \quad \hat{H}_{\pi\nu} = \sum_t \kappa^{\pi\nu}_t (-)^t \sqrt{2t+1} \big(\hat{Q}^t_\pi \times \hat{Q}^t_\nu\big)^{(0)}, \\ \hat{H}_\eta &= \sum_\alpha \varepsilon_{j_\alpha} a^{\eta\dagger}_\alpha a^\eta_\alpha + \sum_r G_r \sqrt{2r+1} \big(A^{r\dagger}_\eta \times \tilde{A}^r_\eta\big)^{(0)} + \sum_t \kappa_t (-)^t \sqrt{2t+1} \big(\hat{Q}^t_\eta \times \hat{Q}^t_\eta\big)^{(0)}, \end{aligned} \tag{40}$$

where ε_{j_α} are single-particle energies and G_r, κ_t, and $\kappa^{\pi\nu}_t$ are adjustable parameters optimized by experimental data of energy levels. For the pairing forces, the structure coefficients in the uncoupled representation are fixed as

$$o_{\alpha\beta\gamma\delta} = y(j_\alpha j_\beta r) y(j_\gamma j_\delta r) C^{J\,m_\alpha+m_\beta}_{j_\alpha m_\alpha, j_\beta m_\beta} C^{J\,m_\alpha+m_\beta}_{j_\gamma m_\gamma, j_\delta m_\delta}. \tag{41}$$

Here $y(j_\alpha j_\beta r)$ are simply the structure coefficients of operator $A^{r\dagger}$ in Eq. (40); while, for the proton-neutron multipole-multipole interactions, the structure coefficients have the same form of Eq. (39), with the operator Q^t defined in Eq. (40). The $(\hat{Q}^t \times \hat{Q}^t)^{(0)}$ between like nucleons is in the form of multipole pairing interactions plus single-particle terms. By using

$$\begin{aligned} &\langle \zeta' M' | a^\dagger_\alpha a_\beta a^\dagger_\gamma a_\delta | \zeta M \rangle \\ &= \langle \zeta' M' | a^\dagger_\alpha \{a_\beta, a^\dagger_\gamma\} a_\delta - a^\dagger_\alpha a^\dagger_\gamma a_\beta a_\delta | \zeta M \rangle \\ &= \delta_{\beta\gamma} f_{\alpha\delta} - g_{\alpha\gamma\delta\beta} \end{aligned} \tag{42}$$

we obtain

$$\begin{aligned} &\langle \zeta' M' | (-)^t \sqrt{2t+1} \big(\hat{Q}^t \times \hat{Q}^t\big)^{(0)} | \zeta M \rangle \\ &\quad = o_{\alpha\beta\gamma\delta}(\delta_{\beta\gamma} f_{\alpha\delta} - g_{\alpha\gamma\delta\beta}), \end{aligned}$$

where

$$\begin{aligned} o_{\alpha\beta\gamma\delta} &= (-)^{j_\beta+m_\alpha+j_\delta+m_\delta} q(j_\alpha j_\beta t) q(j_\gamma j_\delta t) \\ &\quad \times C^{t\,m_\alpha-m_\beta}_{j_\alpha m_\alpha, j_\beta -m_\beta} C^{t\,m_\beta-m_\alpha}_{j_\gamma m_\gamma, j_\delta -m_\delta}. \end{aligned} \tag{43}$$

TABLE I. Maximal dimensions of the Hamiltonian matrices for J-NPA and the dimension of M-scheme NPA, with SD-pair configuration and the number of pairs $N_\pi = N_\nu$. The nucleon-pair configuration in the NPA version of this paper takes that of the J-NPA.

$N_\pi = N_\nu$	1	2	3	4	5	6
J-NPA	3	17	61	216	601	1530
M-NPA	8	65	350	1452	4942	14518

C. Computational superiority

In this subsection, we perform numerical experiments to demonstrate the computational power of our approach, in the costs of both RAM and CPU. This is done by calculating low-lying spectra of a few even-even nuclei in the SD-pair subspace with three approaches, the traditional J-NPA [10], the M-NPA [19], and the approach suggested in this paper, for systems with valence proton pairs in the 50–82 major shell, and valence neutron pairs in the 82–126 major shell, and the number of pairs $N_\pi = N_\nu$. We take both forms of the Hamiltonian, i.e., the monopole and quadrupole pairing plus quadrupole-quadrupole interactions, corresponding to Eq. (40) with $r = 0,\ 2$, and $t = 2$, and the effective interactions in the form of Eq. (35).

In Table I we list maximal dimensions of the Hamiltonian matrices for J-NPA and the dimension of M-scheme NPA, with SD-pair configuration and the number of pairs $N_\pi = N_\nu$. The approach suggested in this paper takes the same basis states as the J-NPA, in which the dimensions of matrices are one order smaller than that of the M-NPA when $N_\pi = N_\nu \geqslant 6$, thus the RAM cost is reduced by two orders or more in our approach compared to that in the M-NPA. This simplicity is crucial if one has to consider nucleon pairs with higher spins other than the SD pairs, because in those cases the model space is considerably expanded and the storage of the Hamiltonian matrix becomes an issue.

In Fig. 1, we plot the serial CPU time of our numerical experiments. One sees that the CPU-time cost of the M-NPA approach is systematically lower than that of the traditional J-NPA; in particular, the CPU-time cost of the M-NPA approach is lower by about two orders in the case of $N_\pi = N_\nu \geqslant 4$, which is consistent with Fig. 2 of Ref. [19] and the discussions therein. In Fig. 1(a), one sees that the CPU time of the approach suggested in this paper is further reduced by one order or more for the case of $N_\pi = N_\nu \geqslant 4$, with the Hamiltonian in the form of the phenomenological pairing plus multipole-multipole interactions. This improvement is given partially by the fact that in the present approach only matrix elements with specific projection are necessary while in the M-NPA one has to calculate those with all possible projections; more details of relevant discussion are given in Appendix A.

The CPU times for the new approach with the effective two-body interactions are plotted in Fig. 1(b). One sees that the CPU times in this case are very close to those with the simple phenomenological interaction. By contrast, the CPU times for both J-NPA and M-NPA increase by about two orders if one use the effective interaction rather than the simple phenomenological pairing plus multipole-multipole interaction. This is another very important superiority of the present approach. The key improvement accounting for this superiority is that the noncollective matrix elements, $g_{\alpha\beta\gamma\delta}$ and $f_{\alpha\beta}$, are given in a unified way by Eqs. (32) and (33), and then the matrix elements of $\hat{H}$ are calculated with a sum of those noncollective values according to Eqs. (11) and (12). This is similar to the technique of the coefficients of fractional parentage in the traditional J-scheme shell model calculations.

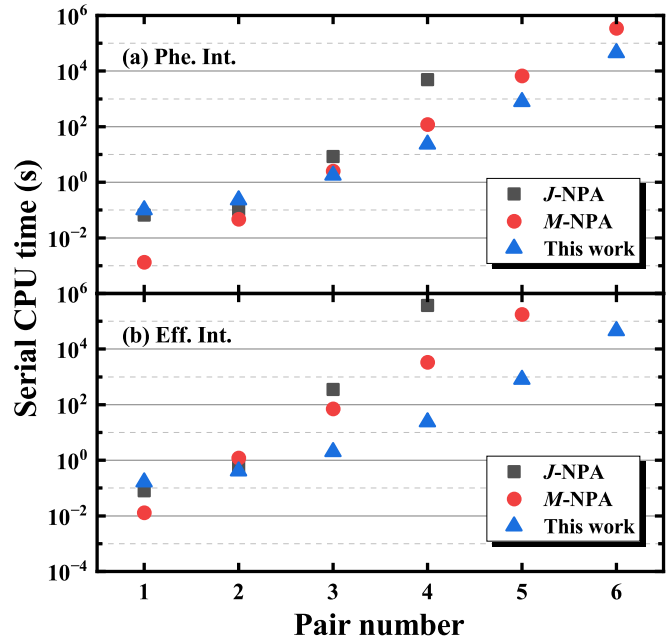

FIG. 1. Serial CPU time of the SD nucleon-pair truncated configuration versus valence nucleon pair numbers $N_\pi = N_\nu$, with valence proton pairs in the 50–82 major shell, and valence neutron pairs in the 82–126 major shell. In panel (a) we use the phenomenological pairing plus quadrupole-quadrupole interactions, and in panel (b) we use the effective interactions. The results of the traditional J-NPA of Refs. [10] and the M-NPA of Ref. [19] are presented for comparison. The calculations are carried out on a conventional PC with CPU frequency 4.9 GHz.

V. APPLICATION TO EVEN-EVEN Nd ISOTOPES

In this section we apply our approach to even-even Nd isotopes, from the semimagic ^{142}Nd to the well-deformed ^{152}Nd, with the Hamiltonian assuming a general form of effective interaction defined in Eq. (35).

A. Parameters and model space

Let us first explain the parameters in our calculations. Our single-particle energies, ε_j, are taken from the experimental spectra of ^{133}Sb and ^{133}Sn compiled in the National Nuclear Data Center (NNDC) [22], as shown in Table II. In this case valence protons are in the $2s_{1/2}$, $1d_{3/2}$, $1d_{5/2}$, $0g_{7/2}$, and $0h_{11/2}$ orbits, and valence neutrons are in the $2p_{1/2}$, $2p_{3/2}$, $1f_{5/2}$, $1f_{7/2}$, $0h_{9/2}$, and $0i_{13/2}$ orbits. The two-body effective matrix elements, $V_{JT}(j_\alpha j_\beta j_\gamma j_\delta)$, were obtained by integrating the model-independent low-momentum nucleon-nucleon

TABLE II. Single-particle energies of valence protons (π) and valence neutrons (ν) adopted in this work. These values are taken from the experimental spectra of ^{133}Sb and ^{133}Sn [22].

j_π	$2s_{1/2}$	$1d_{3/2}$	$1d_{5/2}$	$0g_{7/2}$	$0h_{11/2}$	
ϵ_{j_π}	2.990	2.440	0.962	0.000	2.793	
j_ν	$2p_{1/2}$	$2p_{3/2}$	$1f_{5/2}$	$1f_{7/2}$	$0h_{9/2}$	$0i_{13/2}$
ϵ_{j_ν}	1.363	0.854	2.005	0.000	1.561	2.690

interaction [23,24], i.e., $V_{\text{low-}k}$, using the harmonic oscillator eigenfunctions with the oscillator energy $\hbar\omega = 7.87$ MeV.

The effective charges of valence nucleons used in this paper are obtained by the χ^2-fitting procedure, yielding that $e_\pi = 2.53\,e$ and $e_\nu = 1.27\,e$, which are slightly larger than the values adopted in Refs. [25] and [26]. For effective g factors, we use the values $g_{s\pi} = 5.586 \times 0.7\,\mu_N$ and $g_{s\nu} = -3.826 \times 0.7\,\mu_N$ (0.7 is the usual quenching factor in the NSM calculations). The orbital g factors are taken as $g_{l\pi} = 1.0\,\mu_N$ and $g_{l\nu} = 0\,\mu_N$.

Now we elaborate which nucleon pairs are chosen as the building blocks of our model space. The even-even $^{142-152}$Nd chain provides us with a very typical example of excitation modes from seniority-type (^{142}Nd), vibrational (^{144}Nd), transitional (^{146}Nd and ^{148}Nd), and rotational (^{150}Nd and ^{152}Nd) modes. The nucleon-pair structure of optimal collective pairs for these nuclei are expected to be very different, as clarified in Ref. [27]. Hence we utilize both the generalized seniority-like (GS) and the Hartree-Fock (HF) approaches, explained in Appendix C, to obtain the structure coefficients of nucleon pairs. For ^{142}Nd and ^{144}Nd, the neutron-proton interaction is very small because the valence neutron numbers are small. In those cases we use the generalized seniority scheme to extract the structure coefficients of collective pairs. We use S, D, G, and I pairs for both valence protons and neutrons in those two isotopes. For the ^{146}Nd nucleus, there are four valence neutrons, therefore the neutron-proton interaction starts to play a role towards deformation; for this nucleus, our S pair is optimized by assuming the ground state to be S-pair condensation state, as in Eq. (C3), while the non-S pairs are derived from the Hartree-Fock ground state (see Appendix C for a detailed description); for this nucleus the non-S pairs are chosen to be D and G pairs. For ^{148,150,152}Nd isotopes, all pair structures are fixed by nucleon pairs extracted from corresponding deformed Hartree-Fock ground states. More specifically, apart from the dominated S and D pairs, there are two types of G pairs which contribute about 4% to the Hartree-Fock ground state of ^{148}Nd, and we choose the one which contributes relatively more to the Hartree-Fock ground state, with the number of G pairs below 3 for both valence protons and valence neutrons in the calculation; for ^{150,152}Nd isotopes, collective nucleon pairs with largest amplitudes in the Hartree-Fock ground states are S, D, G, and I pairs, respectively, for both valence neutrons and protons. Again we restrict the number of G and I nucleon pairs below 2, individually for both valence neutrons and valence protons, in order to have our model space procurable by a PC (we note that for the number of 8^+ states of ^{152}Nd in such selected configuration space is already 419 243, requiring the storage space over 1 TB). In all cases, the number of nucleon pairs other than SD pairs is restricted to be equal to or less than 2.

B. Calculated results and discussion

In Fig. 2, we plot our calculated energies of low-lying states with the $V_{\text{low-}k}$ shell model Hamiltonian, by using the NPA in the $SDGI$ nucleon-pair configuration (number of nucleon pairs beyond SD pairs below 3 for both valence protons and valence neutrons), and compare them with experimental data. For ^{142}Nd and ^{144}Nd, the calculated excitation energies of 2_1^+ states are close to the experimental values. The general features of yrast states in these two nuclei are well reproduced; in particular, the 2_1^+ state energies are very consistent with experimental data. For ^{142}Nd, the 4_1^+ and 6_1^+ states are nearly degenerate, and the 8_1^+ are relatively high in energy. These yrast states are expected to be "nucleon-pair states" suggested in Ref. [28], and, according to the present calculation,

$$|2_1^+\rangle = 0.98|S^4D\rangle_\pi + \cdots,$$
$$|4_1^+\rangle = 0.98|S^4G\rangle_\pi + \cdots,$$
$$|6_1^+\rangle = 0.97|S^4I\rangle_\pi + \cdots,$$
$$|8_1^+\rangle = 0.93|S^3(D\times I)^{(8)}\rangle_\pi + \cdots,$$

For ^{144}Nd, the calculated excitation energies for the 4_1^+ and 6_1^+ states are sizably lower than corresponding experimental data. For ^{146}Nd, good agreement between the experimental and calculated values is achieved for the low-lying yrast states, up to the high-spin 8_1^+ and 10_1^+ states. For these states the "nucleon-pair state" picture are not applicable. The maxima of overlaps between eigenstates and pair basis states are 0.62, 0.48, 0.38, 0.33, and 0.36, for the 2^+, 4^+, 6^+, 8^+, and 10^+ band states, respectively. For ^{148}Nd and ^{150}Nd, our calculations reproduce the ground band energies very well. Yet, the side bands of these nuclei are not well described in our calculations. For example, the second 0^+ state is even higher than the second 2^+ and 4^+ states, and the energy gaps between the 2^+ and 4^+ states are too small in comparison with experimental data. This is partially understandable, as our pair structure coefficients are derived from the HF ground state. To simulate the side band states, one might need to consider other pairs, as exemplified for ^{68}Se and ^{68}Ge in Ref. [29]. For ^{152}Nd, the moment of inertia for the ground band is about one-half of the experimental value. This disagreement might come from two origins: one is the constraint of number of G and I pairs in the configuration space, and the second is that the $V_{\text{low-}k}$ matrix elements are not properly refined with experimental data in this region.

Our calculated $B(E2)$ and μ values for the yrast states of even-even Nd isotopes are presented in Table III (denoted by "Th"), and are compared with experimental data accessible in the NNDC. For ^{142}Nd, $B(E2; 0_1^+ \to 2_1^+)$ and $\mu(2_1^+)$ are slightly larger than the experimental values, and the calculated E2 transition probabilities between 2_1^+, 4_1^+, 6_1^+, and 8_1^+ states are very close to zero or very small. As the neutron number increases from ^{142}Nd to ^{152}Nd, the $E2$ transition probabilities between 2_1^+, 4_1^+, 6_1^+, and 8_1^+ states, for both calculated and experimental data, become stronger and stronger successively,

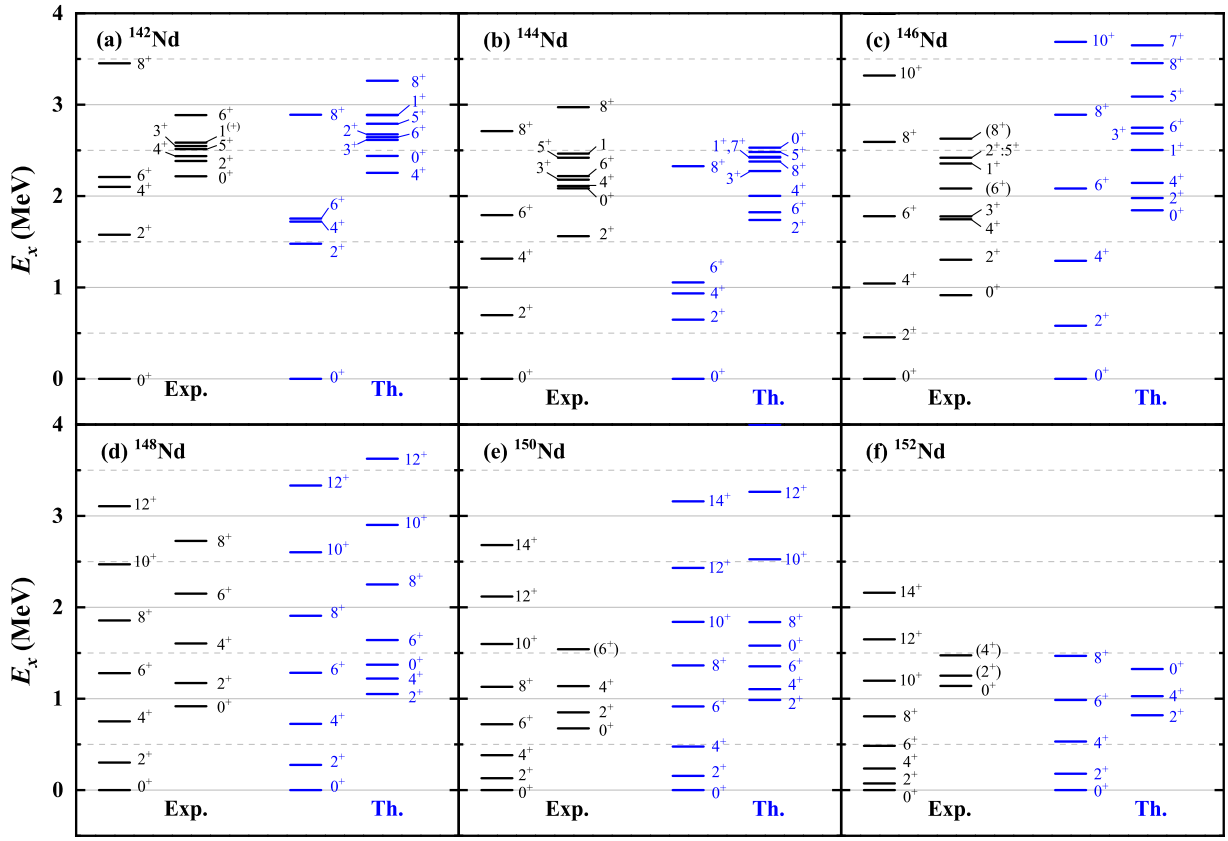

FIG. 2. Low-lying energy spectra for even-even Nd isotopes. The experimental data are extracted from the NNDC [22], and the theoretical results are calculated by using the NPA with $V_{\text{low-}k}$ potential. Refer to the text for details.

TABLE III. Reduced transition probability $B(E2)$ (in $e^2\text{b}^2$) and magnetic moment μ (in ν_N) for low-lying states of even-even $^{142-152}$Nd. The effective charges are $e_\pi = 2.53e$, $e_\nu = 1.27e$, $g_{l\pi} = 1.0\,\mu_N$, $g_{l\nu} = 0\,\mu_N$, $g_{s\pi} = 5.586 \times 0.7\,\mu_N$, $g_{s_\nu} = -3.826 \times 0.7\,\mu_N$. Experimental data are taken from the NNDC [22]. The theoretical values based on the *SDGI*-pair configuration are represented by "Th", and those based on the *SD*-pair configuration are represented by "Th1".

	Expt.	Th	Th1	Expt.	Th	Th1	Expt.	Th	Th1
$B(E2)$	^{142}Nd			^{144}Nd			^{146}Nd		
$0^+ \to 2^+$	0.265(4)	0.463	0.453	0.58(1)	0.489	0.449	0.728(9)	1.11	1.06
$2^+ \to 4^+$		0.001	0.184	0.153(19)	0.162	0.263	0.354(90)	0.665	0.590
$4^+ \to 6^+$		<0.001	0.162	0.157(16)	0.065	0.248		0.638	0.535
$6^+ \to 8^+$		0.063	0.163		0.160	0.252		0.610	0.513
$B(E2)$	^{148}Nd			^{150}Nd			^{152}Nd		
$0^+ \to 2^+$	1.37(2)	2.06	1.85	2.75(7)	2.96	2.32	4.17(24)	3.28	2.20
$2^+ \to 4^+$	0.784(24)	1.13	0.991	1.54(1)	1.54	1.24	1.96(9)	1.72	1.09
$4^+ \to 6^+$	0.685(47)	1.01	0.865	1.41(6)	1.33	1.08	1.57(30)	1.45	0.956
$6^+ \to 8^+$	0.596(103)	0.961	0.766	1.34(14)	1.14	0.966		1.33	0.865
μ	^{142}Nd			^{144}Nd			^{146}Nd		
2^+	+1.69(15)	+2.43	+2.41	0.35(3)	−0.309	−0.167	+0.582(14)	+0.581	+0.682
4^+		+5.46	+4.67		−0.934	+2.28	+0.77(10)	+1.31	+1.63
6^+		+6.27	+6.20		−1.75	+4.70		+2.51	+3.40
8^+		+8.92	+7.93		+0.743	+6.61		+4.29	+5.04
μ	^{148}Nd			^{150}Nd			^{152}Nd		
2^+	+0.73(3)	+1.06	+1.14	+0.84(4)	+0.786	+1.09		+1.00	+1.10
4^+	+1.4(2)	+2.17	+2.38	+1.8(3)	+1.65	+2.20		+2.07	+2.17
6^+	+1.6(3)	+3.35	+3.68	+2.1(4)	+2.82	+3.31		+3.40	+3.15
8^+		+4.68	+4.98	+4.5(10)	+4.29	+4.38		+4.78	+4.02

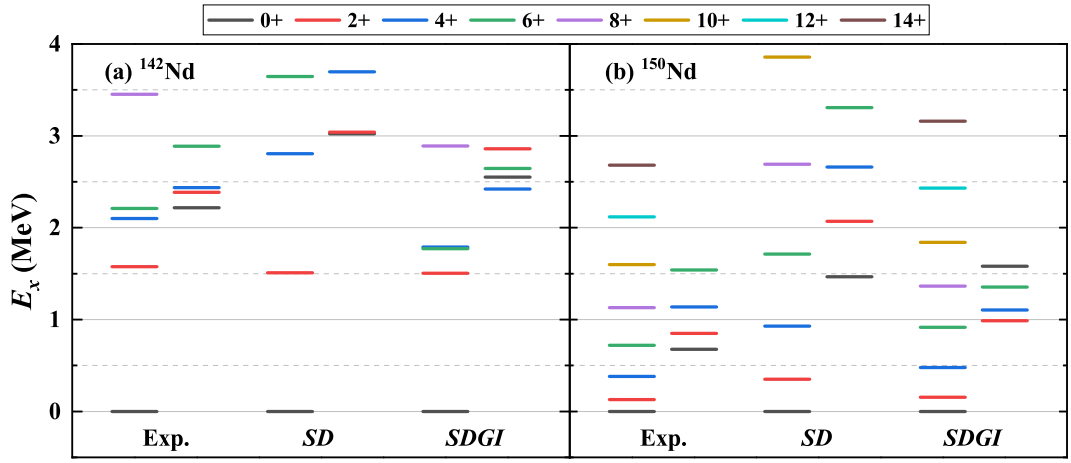

FIG. 3. Low-lying energy levels of (a) semimagic ^{142}Nd and (b) well deformed ^{150}Nd. "*SD*" represents the NPA calculation by using *SD* nucleon pairs, "*SDGI*" represents that by using *SDGI* nucleon pairs. Experimental data are taken from the NNDC [22].

and this pattern is well described by our NPA calculations. Similarly, the general feature of the magnetic moments is well reproduced in the NPA calculation, with an exception that the calculated $\mu(2_1^+)$ of ^{144}Nd has a different sign than the experimental value.

C. Important role of *G* and *I* nucleon pairs

In most previous NPA calculations, e.g., [25,26], the model spaces are constructed by only collective *S* and *D* pairs. It has been well known for a long time that collective *G* and *I* pairs are also important for well deformed nuclei. This was recently revisited in Refs. [27,29]. As a byproduct of our NPA calculation, we investigate the role of *G* and *I* nucleon pairs for even-even $^{142-152}$Nd isotopes. This can be easily performed by the NPA calculations with only *SD* nucleon pairs. In this *SD* nucleon-pair approximation, the structure coefficients of the *S* and *D* pairs are taken the same as above.

In Fig. 3, we plot our calculated low-lying energy levels for ^{142}Nd and ^{150}Nd by using the NPA, in both the *SD* nucleon-pair space, denoted by "*SD*", and the *SDGI* nucleon-pair space in Fig. 2, denoted by "*SDGI*". For the semimagic ^{142}Nd, good agreement between the two calculations is seen for the excitation energies of the 2_1^+ state, while excitation energies for other states of *SD*-pair calculation are much higher than those of the *SDGI*-pair calculation. For ^{150}Nd, the rotational behavior is reproduced in both calculations; however, the moment of inertia in the *SD*-pair calculation is much lower than the experimental value. This clearly demonstrate the important roles played by *G* and *I* nucleon pairs for deformed nuclei. In Table III we present calculated $B(E2)$ and μ values in the *SD*-pair configuration (see the column "Th1"). In general, $B(E2)$ values of the 'Th1" column are smaller than those of the "Th" column, with few exceptions. On the other hand, the μ values of the "Th1" column are larger than those of the "Th" column. Overall, the electromagnetic properties obtained from the *SDGI*-pair space are closer to reality.

VI. SUMMARY AND DISCUSSION

In this paper, we have suggested a new version of the NPA to the nuclear shell model. In our new formulation, we take the *J*-NPA basis states, on the one hand, and make use of the commutators of the *M*-NPA in calculations for the one- and two-body matrix elements as well as the overlaps, on the other hand. The advantages for this new development of the NPA, as explained in the text and exemplified by even-even Nd isotopes, are that the costs of CPU and RAM are reduced substantially, in comparison with all previous *M*-NPA calculations, while the simplicity of the *J*-scheme NPA is reserved. Therefore, this new version of the NPA is much more realizable to study the low-lying structure of medium and heavy nuclei.

One of key improvements in this new version of the NPA is that one needs reduced matrix elements with only one specific projection, while one needs those with all possible projections in all previous *M*-NPAs. Numerical experiments have demonstrated that our new approach reduces the CPU time by more than one to two orders of magnitude for $N_\pi = N_\nu \geqslant 4$, in comparison with the *M*-scheme approaches of Refs. [18,19]. Furthermore, calculations with the shell model Hamiltonian in the form of effective interactions are as simple as those with the simple pairing plus multipole-multipole interactions in this new approach, owing to a technique similar to the coefficient of fractional parentage in the traditional *J*-scheme shell model calculation. Therefore we call our approach the state-of-the-art version of the NPA.

To exemplify our approach, we study the low-lying states of even-even $^{142-152}$Nd isotopes. These isotopes were recently studied by using the NPA [25], but with monopole and quadrupole pairing plus quadrupole-quadrupole interaction, in the *SD* nucleon pair configuration. In this paper we use the shell model Hamiltonian derived from the $V_{\text{low-}k}$ potential. Our nucleon-pair structure coefficients are fixed by the generalized seniority approach for ^{142}Nd and ^{144}Nd, by the Hartree-Fock ground state for ^{148}Nd, ^{150}Nd, and ^{152}Nd, and by the generalized seniority approach for *S* pairs of ^{146}Nd and by the Hartree-Fock ground state for non-*S* pairs of ^{146}Nd.

We use the *SDGI* nucleon pairs as the building blocks of our wave functions, with the constraint that the number of pairs beyond *SD* pairs is below 2. For the first time, the NPA calculations reproduce the general features of low-lying states for rare-earth isotopes, including seniority-type, vibrational, transitional, and rotational modes, without any refinements of $V_{\text{low-}k}$ matrix elements, and on the same footing. As a byproduct of this exemplification, we investigate the important role played by the collective G and I pairs. Because the NPA calculation with the $V_{\text{low-}k}$ effective interactions provides us with a reasonable description of even-even $^{142-152}$Nd isotopes, in future it would be desirable to refine carefully the $V_{\text{low-}k}$ effective interactions by using experimental data of rare-earth nuclei, including both even-even and odd-mass Nd isotopes.

ACKNOWLEDGMENTS

One of the authors (C.M.) is grateful to Prof. Y. Lei, Prof. G. J. Fu, and Prof. Y. Y. Cheng for discussions. We thank the National Natural Science Foundation of China (Grants No. 11975151, No. 12375114, and No. 11961141003) and the MOE Key Lab for Particle Physics, Astrophysics and Cosmology for financial support.

APPENDIX A: CLEBSCH-GORDAN COEFFICIENT IN EQ. (7)

In this Appendix, we discuss an interesting feature of the Clebsch-Gordan coefficient used in Eq. (7). In Eq. (7) it would be very desirable to fix the values of M, μ, and M' in advance, and once for all.

Below we demonstrate how this can be done in our NPA calculations. Let us first discuss the case of an odd-nucleon system where both J and J' are half-integers; in this case we fix $\mu = 0$ and $M = M' = 1/2$, and it suffices to prove that the Clebsch-Gordan coefficient $C^{J\frac{1}{2}}_{J'\frac{1}{2},t0}$ is always nonzero, once J, J', and t satisfy the triangle rule of three vectors. This proof is straightforward. The basic idea is to use recursive relations and fundamental symmetry properties of the CG coefficients, and to see that $C^{J\frac{1}{2}}_{J'\frac{1}{2},t0}$ is proportional to $C^{t0}_{J'\frac{1}{2},J\frac{-1}{2}}$ and $C^{t0}_{J'\frac{-1}{2},J\frac{1}{2}}$. If $C^{J\frac{1}{2}}_{J'\frac{1}{2},t0} = 0$ it means that both $C^{t0}_{J'\frac{1}{2},J\frac{-1}{2}}$ and $C^{t0}_{J'\frac{-1}{2},J\frac{1}{2}}$ are zero. On the other hand, $C^{t0}_{J'\frac{1}{2},J\frac{-1}{2}} = C^{t0}_{J'\frac{-1}{2},J\frac{1}{2}} = 0$ yields all $C^{JM}_{J'M',t\mu} = 0$, according to recursive formula of the Clebsch-Gordan coefficient with the same $J'tJ$. Therefore one needs only matrices with the smallest magnetic number in this version of the NPA. In contrast, in all previous M-NPA [18,19], the matrix elements with all possible magnetic numbers are necessary in calculations. This is one of the advantages in this new version of the NPA.

For the case of an even system, the situation is similar, but with a slight difference. In this case both J and J' are integers, thus $C^{J0}_{J'0,t0} = 0$ for $J + J' + t$ odd. In this situation one sees that $C^{J0}_{J',1;t,-1}$ is always nonzero. Therefore, in our calculation we take $M = M' = 0$ if $J + J' + t$ is even, or $M' = -\mu = 1$ and $M = 0$ if $J + J' + t$ is odd. Again we do not need to calculate matrix elements of any other M, M', and μ.

APPENDIX B: SIMPLE CASES OF THE CONTRACTION

In this Appendix, we present some simple results of Eqs. (19) and (20). For the case of two-pair creation operators and one annihilation operator, we have

$$P'_1P^\dagger_1P^\dagger_2|0\rangle = (\mathscr{P}^\dagger_1 + \mathscr{P}^\dagger_2 + \mathscr{P}^\dagger_{1,2})|0\rangle = \mathcal{B}^\dagger|0\rangle,$$

where the pair structure coefficient matrix b for $\mathcal{B}^\dagger$ equals

$$b = 4(p_1p'_1p_2 + p_2p'_1p_1) - 2[\text{tr}(p_1p'_1)p_2 + \text{tr}(p_2p'_1)p_1]. \tag{B1}$$

For the case of three-pair creation operators and one annihilating operator, we have

$$P'_1P^\dagger_1P^\dagger_2P^\dagger_3|0\rangle = (P^\dagger_2\mathscr{P}^\dagger_1 + P^\dagger_1\mathscr{P}^\dagger_2 + P^\dagger_1\mathscr{P}^\dagger_3 + \mathscr{P}^\dagger_{1,2}P^\dagger_3 + P^\dagger_2\mathscr{P}^\dagger_{1,3} + P^\dagger_1\mathscr{P}^\dagger_{2,3})|0\rangle = \mathcal{Q}^\dagger|0\rangle,$$

with

$$\begin{aligned}\mathfrak{q}_{\alpha\beta\gamma\delta} = 4\big[&\big(p_1p'_1p_2 + p_2p'_1p_1 - \tfrac{1}{2}\text{tr}(p_1p'_1)p_2\big)_{\alpha\beta}p^{(3)}_{\gamma\delta} + \big(p_1p'_1p_3 + p_3p'_1p_1 - \tfrac{1}{2}\text{tr}(p_3p'_1)p_1\big)_{\alpha\beta}p^{(2)}_{\gamma\delta}\\ &+\big(p_2p'_1p_3 + p_3p'_1p_2 - \tfrac{1}{2}\text{tr}(p_2p'_1)p_3\big)_{\alpha\beta}p^{(1)}_{\gamma\delta}\big].\end{aligned} \tag{B2}$$

For an odd-nucleon system, there are in total three cases. In the first case there are one-pair and an unpaired nucleon creation operators, with a one-particle annihilation operator on the left-hand side; and in this case we have

$$a'a^\dagger P^\dagger_1|0\rangle = (\{a', a^\dagger\}P^\dagger_1 - a^\dagger[a', P^\dagger_1])|0\rangle = \mathcal{B}^\dagger|0\rangle, \quad \text{with } b = (s'^\top s)p_1 - ss'^\top p_1 - p_1s's^\top. \tag{B3}$$

In the second case there are two-pair and an unpaired nucleon creation operators, with a one-particle annihilation operator on the left-hand side; and in this case we have

$$a'a^\dagger P^\dagger_1P^\dagger_2|0\rangle = (\{a', a^\dagger\}P^\dagger_1P^\dagger_2 - a^\dagger[a', P^\dagger_1]P^\dagger_2 - a^\dagger P^\dagger_1[a', P^\dagger_2])|0\rangle = \mathcal{Q}^\dagger|0\rangle,$$

with

$$\mathfrak{q}_{\alpha\beta\gamma\delta} = (s'^\top s)p^{(1)}_{\alpha\beta}p^{(2)}_{\gamma\delta} - (ss'^\top p_1 + p_1s's^\top)_{\alpha\beta}p^{(2)}_{\gamma\delta} - (ss'^\top p_2 + p_2s's^\top)_{\alpha\beta}p^{(1)}_{\gamma\delta}. \tag{B4}$$

In the third case, there are two-pair and an unpaired nucleon creation operators, with a one-pair annihilation operator on the left hand side; in this case we have

$$P_1' a^\dagger P_1^\dagger P_2^\dagger |0\rangle = (a^\dagger \mathscr{P}_1^\dagger + a^\dagger \mathscr{P}_2^\dagger + a^\dagger \mathscr{P}_{1,2}^\dagger + a_1^\dagger P_2^\dagger + a_2^\dagger P_1^\dagger)|0\rangle = \mathcal{T}^\dagger|0\rangle,$$

with

$$\mathfrak{t}_{\alpha\beta\gamma} = 4s_\alpha\left[\left(p_1 p_1' p_2 - \tfrac{1}{2}\mathrm{tr}(p_1 p_1')p_2\right)_{\beta\gamma} + \left(p_2 p_1' p_1 - \tfrac{1}{2}\mathrm{tr}(p_2 p_1')p_1\right)_{\beta\gamma}\right] + 4(p_1 p_1' s)_\alpha p^{(2)}_{\beta\gamma} + 4(p_2 p_1' s)_\alpha p^{(1)}_{\beta\gamma}. \quad \text{(B5)}$$

These results are useful in writing computer codes of this version of the NPA.

APPENDIX C: OPTIMIZATION OF NUCLEON-PAIR STRUCTURE

In this Appendix we summarize how to obtain the nucleon-pair structure coefficients in the NPA calculations.

In many NPA calculations, the pair-structure coefficients, $y(j_\eta j_\eta' r)$, of the collective pairs are obtained by the broken-pair approximation [5]. For a given NSM Hamiltonian, one solves the BCS equation to obtain the empty and occupied amplitudes, u_{j_η} and v_{j_η}, for each orbit j_η. Then the structure coefficients of the S pair is given by

$$y(j_\eta j_\eta' 0) = \delta_{j_\eta j_\eta'}\sqrt{2j_\eta + 1}\frac{v_{j_\eta}}{u_{j_\eta}}, \quad \text{(C1)}$$

corresponding to the number-projected BCS wave function. The structure of non-S pairs is subsequently determined by using phonon excitation. For example, one derives the D pair using the commutator $D^\dagger = \frac{1}{2}[Q, S^\dagger]$, and obtains the structure coefficients

$$y(j_\eta j_\eta' 2) = \frac{1}{2}q(j_\eta j_\eta' 2)\left[\frac{y(j_\eta j_\eta 0)}{\sqrt{2j_\eta + 1}} + \frac{y(j_\eta' j_\eta' 0)}{\sqrt{2j_\eta' + 1}}\right], \quad \text{(C2)}$$

where $q(j_\eta j_\eta' 2)$ express the inherent structure of the quadrupole phonon Q. These operations are performed for protons and neutrons individually. Clearly, the proton-neutron correlations are not considered.

Alternatively, in some previous works, the structure of the collective pairs is optimized using the generalized seniority-like (GS) approach [30]. First, the structure of the S pair is obtained by minimizing the expectation value of Hamiltonian in a pair-condensation state, resorting to a nonlinear optimization like the Levenberg-Marquardt algorithm [31,32]. For an open-shell nucleus, $y(j_\pi j_\pi' 0)$ and $y(j_\nu j_\nu' 0)$ are obtained by optimizing

$$\frac{\langle (S_\pi)^{N_\pi}(S_\nu)^{N_\nu}|\hat{H}|(S_\pi)^{N_\pi}(S_\nu)^{N_\nu}\rangle}{\langle (S_\pi)^{N_\pi}(S_\nu)^{N_\nu}|(S_\pi)^{N_\pi}(S_\nu)^{N_\nu}\rangle}. \quad \text{(C3)}$$

Second, for the structure coefficients of non-S pairs, one diagonalizes the Hamiltonian matrix in a subspace spanned by the one-broken-pair states, $(a^\dagger_{j_\pi} \times a^\dagger_{j_\pi'})^{(r)}(S_\pi^\dagger)^{N_\pi - 1}(S_\nu^\dagger)^{N_\nu}|0\rangle$, for non-$S$ proton pairs as an example. The yrast state in this small space is a superposition of the broken pair states,

$$\sum_{j_\pi \leqslant j_\pi'} c_r(j_\pi j_\pi')\left(a^\dagger_{j_\pi} \times a^\dagger_{j_\pi'}\right)^{(r)}(S_\pi^\dagger)^{N_\pi - 1}(S_\nu^\dagger)^{N_\nu}|0\rangle, \quad \text{(C4)}$$

and we take $y(j_\pi j_\pi' r) = c_r(j_\pi j_\pi')(1 + \delta_{j_\pi j_\pi'})/2$. If the monopole-monopole contribution is absent from the neutron-proton interaction, as in the case of the phenomenological Hamiltonian, the above procedure can be done for protons and neutrons independently. Again, the proton-neutron correlations, important for rotational nuclei, are not considered in the GS approach.

The third method is as follows. One also obtains the structure coefficients of transitional and rotational nuclei from a Hartree-Fock (HF) Slater determinant, as summarized in Ref. [33]. One first performs the HF calculation in the NSM model space with an NSM effective interaction [34]. The HF single-particle states obtained from this calculation are represented by a transformation from the original NSM single-particle states, $U_{i\alpha}$ with i and $\alpha = \{j_\alpha, m_\alpha\}$ being the indices of the HF and the NSM states, respectively. The HF ground state with $2N$ of valence protons (or neutrons) can be written as a pair condensate:

$$\begin{aligned}|\varphi_{\mathrm{HF}}\rangle &= (N!)^{-1}\left(\sum_{ik\alpha\beta} g_{ik}U_{i\alpha}U_{k\beta}a^\dagger_\alpha a^\dagger_\beta\right)^N |0\rangle \\ &= (N!)^{-1}(B^\dagger)^N|0\rangle, \end{aligned} \quad \text{(C5)}$$

where $g_{12} = g_{34} = \cdots = g_{(2N-1)(2N)} = 1$ and other $g_{ij} = 0$. Due to the symmetry breaking in the HF calculation, the condensate pair $B^\dagger$ does not possess good spin. On the other hand, one can project out pairs with good spin (and parity) from the deformed HF pair,

$$B^{(J)\dagger}_{MK} = \sum_{j_\alpha, j_\beta} y_{JK}(j_\alpha j_\beta)(a^\dagger_{j_\alpha} \times a^\dagger_{j_\beta})^{(J)}_M, \quad \text{(C6)}$$

where

$$y_{JK}(j_\alpha j_\beta) = \sum_{ikm_\alpha m_\beta} g_{ik}(U_{i\alpha}U_{k\beta} - U_{k\alpha}U_{i\beta})C^{JK}_{j_\alpha m_\alpha j_\beta m_\beta}. \quad \text{(C7)}$$

For a given angular momentum J, we diagonalize the norm matrix

$$N^{(JM)}_{KK'} = \langle 0|B^{(J)}_{MK}B^{(J)\dagger}_{MK'}|0\rangle, \quad \text{(C8)}$$

leading to the unique pairs with rotational invariance. The nonzero eigenvalues of $N^{(JM)}_{KK'}$ are amplitudes of these pairs, reflecting their contribution in the deformed HF pair. It has been demonstrated that the nucleon pairs obtained in this way provide us with a good description of low-lying states for deformed nuclei [27].

[1] M. G. Mayer, Phys. Rev. **75**, 1969 (1949).
[2] J. H. D. Jensen, H. E. Sueß, and O. Haxel, Naturwissenschaften **36**, 155 (1949).
[3] I. Talmi, Nucl. Phys. A **172**, 1 (1971).
[4] F. Q. Luo and M. A. Caprio, Nucl. Phys. A **849**, 35 (2011).
[5] K. Allaart, E. Boeker, G. Bonsignori *et al.*, Phys. Rep. **169**, 209 (1988); Y. K Gambhir, S. Haq, G. Bonsignori, M. Savoai, and Y. K. Gambhir, Ann. Phys. (N.Y.) **133**, 154 (1981).
[6] J. N. Ginocchio, Ann. Phys. (NY) **126**, 234 (1980).
[7] C. L. Wu, D. H. Feng, X. G. Chen, J. Q. Chen, and M. W. Guidry, Phys. Rev. C **36**, 1157 (1987).
[8] C. L. Wu, D. H. Feng, and M. Guidry, Adv. Nucl. Phys. **21**, 227 (1994).
[9] L. J. Liotta and C. Pomar, Nucl. Phys. A **362**, 137 (1981).
[10] J. Q. Chen, Nucl. Phys. A **626**, 686 (1997); Y. M. Zhao, N. Yoshinaga, S. Yamaji, J. Q. Chen, and A. Arima, Phys. Rev. C **62**, 014304 (2000).
[11] A. Arima and F. Iachello, Phys. Rev. Lett. **35**, 1069 (1975); Ann. Phys. (N.Y.) **99**, 253 (1976); **111**, 201 (1978); **115**, 325 (1978); **123**, 468 (1979).
[12] T. Otsuka, A. Arima, F. Iachello, and I. Talmi, Phys. Lett. B **76**, 139 (1978).
[13] J. N. Ginocchio and C. W. Johnson, Phys. Rep. **264**, 153 (1996).
[14] N. Yoshinaga, T. Mizusaki, A. Arima, and Y. D. Devi, Prog. Theor. Phys. Suppl. **125**, 65 (1996).
[15] Y. M. Zhao and A. Arima, Phys. Rep. **545**, 1 (2014).
[16] G. J. Fu, Y. Lei, Y. M. Zhao, S. Pittel, and A. Arima, Phys. Rev. C **87**, 044310 (2013).
[17] Y. Y. Cheng, Y. M. Zhao, and A. Arima, Phys. Rev. C **97**, 024303 (2018).
[18] B. C. He, L. Li, Y. A. Luo, Y. Zhang, F. Pan, and J. P. Draayer, Phys. Rev. C **102**, 024304 (2020).
[19] Y. Lei, Y. Lu, and Y. M. Zhao, Chin. Phys. C **45**, 054103 (2021).
[20] T. Mizusaki and T. Otsuka, Prog. Theor. Phys. Suppl. **125**, 97 (1996).
[21] K. Kumar, Prog. Part. Nucl. Phys. **9**, 233 (1983).
[22] National Nuclear Data Center, https://www.nndc.bnl.gov/.
[23] S. Bogner, T. T. S. Kuo, L. Coraggio, A. Covello, and N. Itaco, Phys. Rev. C **65**, 051301(R) (2002).
[24] S. K. Bognera, T. T. S. Kuo, and A. Schwenk, Phys. Rep. **386**, 1 (2003).
[25] B. C. He, S. Y. Zhang, L. Li, Y. A. Luo, Y. Zhang, F. Pan, and J. P. Draayer, Phys. Rev. C **105**, 044332 (2022).
[26] L. Y. Jia, H. Zhang, and Y. M. Zhao, Phys. Rev. C **75**, 034307 (2007); **76**, 054305 (2007).
[27] G. J. Fu and C. W. Johnson, Phys. Rev. C **104**, 024312 (2021).
[28] Y. Y. Cheng, H. Wang, J. J. Shen, X. R. Zhou, Y. M. Zhao, and A. Arima, Phys. Rev. C **100**, 024321 (2019).
[29] G. J. Fu and C. W. Johnson, Phys. Lett. B **809**, 135705 (2020).
[30] Z. Y. Xu, Y. Lei, Y. M. Zhao, S. W. Xu, Y. X. Xie, and A. Arima, Phys. Rev. C **79**, 054315 (2009).
[31] K. Levenberg, Quart. Appl. Math. **2**, 164 (1944).
[32] D. W. Marquardt, J. Soc. Indust. Appl. Math. **11**, 431 (1963).
[33] F. Iachello and I. Talmi, Rev. Mod. Phys. **59**, 339 (1987).
[34] I. Stetcu and C. W. Johnson, Phys. Rev. C **66**, 034301 (2002).